Role of NH_3 as an intermediate in reduction of NO with CH_4 over sol–gel Pd catalysts on TiO_2

Junko M. Watson, Umit S. Ozkan[*]

Department of Chemical Engineering, The Ohio State University, 140 W. 19th Avenue, Columbus, OH 43210, USA

Abstract

Our previous studies [Catal. Commun., in press; J. Catal., in press] on sol–gel-prepared Pd catalysts for reduction of NO with CH_4 suggested that one of the key surface species for the $NO–CH_4–O_2$ reaction involved NH_x species. In this study, the use of NH_3 as the reducing agent for NO reduction on the Gd–Pd/TiO_2 catalyst was investigated under steady-state conditions. Also, temperature-programmed desorption using mass spectrometry and diffuse reflectance infrared Fourier transform spectroscopy (DRIFTS) were used to study the adsorption/desorption characteristics of NH_3 on Gd–Pd/TiO_2. It was found that NH_3 was effective in reduction of NO on the reduced catalyst in the absence of O_2 at $300\,°C$ (100% NO conversion). This result was consistent with our earlier suggestion that NH_x species formed through the interaction of methane and NO adspecies could act as a reducing agent for Pd–NO species. In the presence of O_2, however, NH_3 oxidation takes place faster than NO reduction and NO conversion decreased. Our NH_3-TPD experiments indicated that the reversible NH_3 adsorption capacity was higher on the reduced catalyst compared to the oxidized catalyst. Also, there was a strong evidence obtained by DRIFTS that adsorbed NH_3 is transformed into monodentate nitrate species on the oxidized catalyst.

1. Introduction

The selective catalytic reduction (SCR) using NH_3 is known to be the most widely applied technology to reduce NO_x in the presence of O_2 for stationary combustion sources. The industrial catalyst systems, which are based on $V_2O_5–TiO_2$ (anatase), have been investigated extensively due to their high effectiveness in NO reduction by NH_3 and their high resistance to SO_2 poisoning [1–5]. One of the mechanisms proposed earlier for the NH_3-SCR reactions is an Eley–Rideal mechanism where strongly adsorbed NH_3 and gaseous NO react [6]. However, there are different proposals for the type of ammonia activation sites and the nature of adsorbed species. In elucidation of reaction mechanisms, spectroscopic characterization such as isotopic labeling, in situ FTIR, TPD, and ESR have been used in recent years [2,7–11]. In the SCR reactions, direct oxidation of ammonia has been found to play an important role [8,12] and the activity and selectivity of the NO reduction reaction cannot be considered alone without investigating the role of ammonia oxidation.

More recently, the use of hydrocarbons, particularly CH_4, has been investigated as a reducing agent for NO reduction reaction in place of NH_3, use of which has lingering environmental and economic concerns.

* Corresponding author. Tel.: +1-614-292-6623;
fax: +1-614-292-3769.
E-mail address: ozkan.1@osu.edu (U.S. Ozkan).

Methane is considered to be an attractive replacement for NH_3 because it is the most abundant and inexpensive form of hydrocarbon in natural gas; however, it is also the most stable molecule among alkanes, thus most difficult to activate. Noble metals have been investigated heavily for catalytic combustion of hydrocarbons [13,14]. Among noble metals, palladium and platinum are widely used in oxidation applications such as three-way catalysts and methane combustion. The type of catalysts that are most studied for the CH_4–NO reaction is metal-exchanged zeolite catalysts [15–17].

Use of FTIR has been demonstrated to be a powerful tool for elucidation of possible mechanisms for the NO–CH_4–O_2 reaction in recent years. Among the proposed mechanisms for the reaction, common reaction steps proposed to be involved over metal-exchanged zeolitic catalysts are formation of adsorbed NO_2, activation of CH_4 by adsorbed NO_2, and formation of nitromethane (CH_3NO_2) [17–20].

Previously we have reported titania-supported Pd catalysts to be effective for the reduction of NO to N_2 with high selectivity to N_2 [21–23]. The incorporation of lanthanide elements such as Gd was found to improve the oxygen tolerance of the catalysts [23]. The mechanistic aspects of NO–CH_4 reactions were studied using isotopic labeling techniques under both steady-state and transient conditions [21]. From a series of unsteady-state and steady-state isotopic labeling studies that used various labeled species such as $^{15}N^{16}O$, $^{15}N^{18}O$, $^{13}CH_4$, $^{18}O_2$, it was concluded that N_2 was formed through direct participation of CH_4 possibly through a methyl nitrosyl type intermediate, whereas N_2O formation was mainly a result of NO decomposition reaction [21]. Also, steady-state oscillations were used as a probe to gain insight into the reaction network and it was found that the oxidation state of the active metal determined the extent of the three different reaction steps, namely, NO reduction with CH_4, direct CH_4 oxidation, and NO decomposition [22].

More recently, we have used in situ diffuse reflectance infrared Fourier transform spectroscopy (DRIFTS) and TPD to investigate possible mechanisms for the NO–CH_4–O_2 reaction over sol–gel-prepared Pd catalysts at lower temperatures [24,25]. The major surface species under NO flow at 300 °C was identified as linear NO adsorbed on palladium.

At lower temperatures, bridged/bidentate nitrate and monodentate nitrate are formed on the support and are seen to be decomposed or transformed to other compounds at higher temperatures. Subsequently, linear NO is formed on Pd sites. There was a strong evidence that CH_4 and NO competitively adsorb on the surface even at room temperature [25].

An interesting feature that emerged through the DRIFTS experiments was the formation of surface ammonia species. When the reduced catalyst surface was exposed to NO and CH_4 under conditions that gave complete NO conversion, bands that correspond to NH_3 coordinated to Lewis acid sites ($\sim$1180/1200 cm^{-1}) were observed. These bands were accompanied by features in the –NH stretching region (3242–3150 cm^{-1}). Interestingly these bands were never present over the oxidized catalyst, or under conditions where the catalyst was inactive for NO reduction. Also, in comparison to the Gd-free catalyst, the NH_3 formation seemed to be much more prominent over the Gd–Pd. Another interesting finding from our earlier study was the apparent interaction between the surface coordinated NH_3 species and linear Pd–NO species. DRIFTS experiments showed that disappearance of the Pd–NO species always coincided with the formation of surface ammonia species. These observations led us to suggest that adsorbed NH_3 could be an important player in the NO reduction scheme. In this paper, we present the findings from our steady-state reaction experiments of the NO–NH_3–O_2 reaction, NH_3-TPD, and NH_3-DRIFTS studies, which were performed to examine the role of NH_3 in the NO–CH_4–O_2 reaction over Gd–Pd/TiO_2.

2. Methods

2.1. Catalyst preparation

Catalysts were synthesized using a modified sol–gel technique in which co-precipitation and sol–gel methods are incorporated as described elsewhere [23]. The metal loadings of the catalysts were 2%Pd/TiO_2 and 1%Gd–2%Pd/TiO_2 by weight percentage. The BET surface area measurement by N_2 adsorption resulted in the specific surface areas of 80 and 79 m^2/g for 2%Pd/TiO_2 and 1%Gd–2%Pd/TiO_2, respectively.

2.2. Reaction studies

The steady-state reaction experiments were performed using a fixed-bed flow reactor (1/4 in. OD) made of stainless steel. The amount of catalyst packed was 69 mg. The feed composition consisted of NO (500–1780 ppm), NH_3 (500–1780 ppm), and O_2 (0.1–2%), in balance He at a flow rate of 45 cm^3 (STP)/min. The reaction temperature was varied between 125 and 400 °C and was controlled by a PID temperature controller (Omega). In each reaction, the sample was pre-reduced using a mixture of 33% H_2 in He at 200 °C for 30 min. The feed and effluent were analyzed on-line using a combination of a gas chromatograph (5890A HP), a chemiluminescence NO–NO_2–NO_x analyzer (Thermo Environmental Instruments, Model 42H), and an IR ammonia analyzer (Siemens Ultramat 5F). The gas chromatograph was equipped with a $10' \times 1/8$ in. Porapaq Q column and an $8' \times 1/8$ in. molecular sieve column to quantify N_2, O_2, and N_2O. In all experiments, nitrogen and carbon balances closed within a 5% margin.

2.3. Catalyst characterization

Temperature-programmed desorption (TPD) experiments were conducted using a TPR/TPD flow system equipped with a thermal conductivity detector (TCD) described elsewhere [21]. The desorption species were monitored by an HP5890GC-MS. A sample (75 mg) was loaded to the U-shaped quartz reactor and calcined in situ in 10% oxygen in balance helium at 500 °C for 1 h followed by flushing in helium for 30 min. Next, the sample was reduced in 33% hydrogen in balance helium at 200 °C for 30 min followed by flushing for 30 min in helium. Then, the catalyst was cooled down to room temperature under helium flow. Adsorption of gas was done at room temperature for 1 h followed by helium flushing for 1 h to remove physically adsorbed gas.

DRIFTS experiments were performed using a Bruker IFS66 equipped with a DTGS detector and a KBr beamsplitter. Catalysts were placed in a sample cup inside a Spectratech diffuse reflectance cell equipped with KBr windows and a thermocouple mount that allowed direct measurement of the surface temperature. Each catalyst was pre-treated in situ either by calcination under 10% oxygen at 400 °C

surface temperature or by reduction under 30% hydrogen in balance helium at 200 °C surface temperature for 30 min. For sequential adsorption at 300 °C surface temperature, background spectra were taken at 300 °C under helium before adsorption gases were introduced. For adsorption spectra obtained at several different temperature levels, background spectra were taken at each temperature level under helium prior to the introduction of adsorption gas. Each spectrum was averaged over 1000 scans in the mid-IR range (400–4000 cm^{-1}) to a nominal 2 cm^{-1} resolution.

3. Results and discussion

3.1. Catalytic activity

The effect of temperature on the NO–NH_3 reaction on reduced 1%Gd–2%Pd/TiO_2 catalyst is shown in Fig. 1. Equal concentrations of 1800 ppm NO and NH_3 were introduced to the fixed-bed reactor at 200, 250, 300, and 400 °C. At 200 °C, NO conversion was 30% with 16% NH_3 conversion. At 250 °C, 100% NO conversion was achieved with 75% NH_3 conversion. The N-containing products were N_2 and N_2O in which 85% N_2 selectivity was achieved at 250 °C. As the reaction temperature was increased, we observed an increase in N_2 selectivity, reaching ~100% at 300 °C. The conversion of NH_3, however, was unaffected by increasing temperature. This seems to suggest that the stoichiometric reaction $4NH_3 + 6NO \rightarrow 5N_2 + 6H_2O$ is in control throughout the temperature range studied. N_2O formation, on the other hand, is a possible side reaction at lower temperatures. Here N_2 selectivity is defined as a fraction of N_2 produced over total N_2 and N_2O produced.

The effect of O_2 concentration in NO–NH_3 reaction was investigated on reduced 1%Gd–2%Pd/TiO_2 at 200 °C as shown in Table 1. NO and NH_3 feed concentrations were kept constant at 1800 ppm while

Table 1
Effect of O_2 on NO–NH_3 reaction (equal concentration of 1800 ppm) on reduced 1%Gd–2%Pd/TiO_2 catalyst

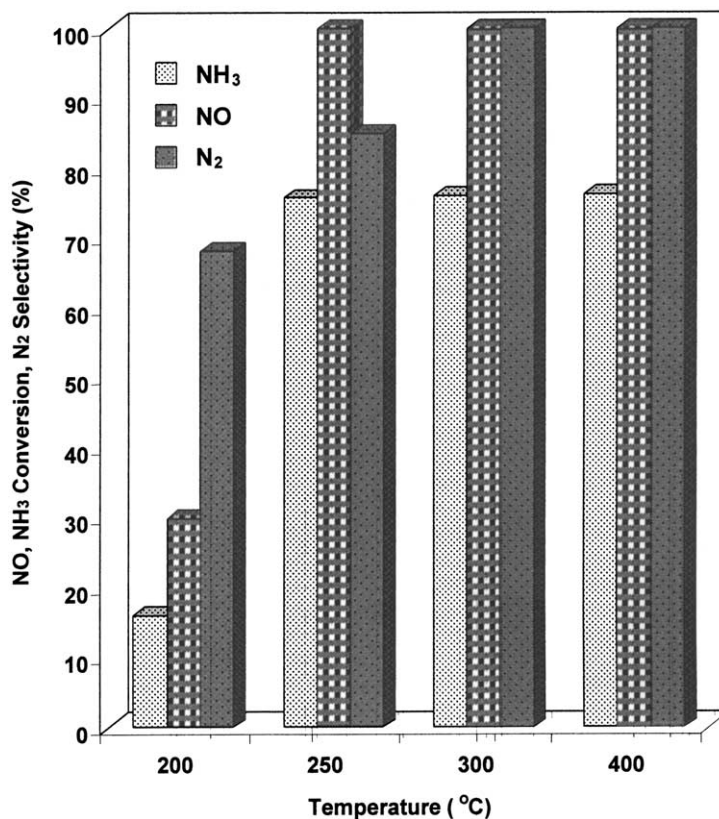| Inlet O_2 (ppm)	0	2000	5000	8000
NO conversion (%)	30	65	68	62
NH_3 conversion (%)	16	77	86	82
NH_3/NO conversion ratio	0.53	1.2	1.3	1.3
N_2 selectivity (%)	68	61	63	48

Fig. 1. Effect of temperature on NO–NH$_3$ reaction (equal concentration of 1800 ppm) on reduced 1%Gd–2%Pd/TiO$_2$ catalyst.

O$_2$ concentration was varied from 0 to 8000 ppm. There was a sharp increase in NH$_3$ conversion from 16 to 77% when 2000 ppm O$_2$ added to the feed. Concurrently, the NO conversion also increased from 30 to 65%. It clearly shows that the presence of O$_2$ helps improve the catalytic activity of NO reduction by NH$_3$ at 200 °C. When O$_2$ level was increased from 2000 up to 8000 ppm, the change in NO or NH$_3$ conversion was relatively small. Table 1 also shows that the ratio of NH$_3$ conversion to NO conversion increased significantly when O$_2$ was added to the feed stream, suggesting that, in the presence of oxygen, direct NH$_3$ oxidation, may also be playing an important role. It should be noted, however, that the "observed" NO reduction may appear to be lower because direct oxidation of NH$_3$ to NO may be boosting the NO concentration in the product stream. The effect of NH$_3$ oxidation was also seen in N$_2$ selectivity,

which decreased in the presence of oxygen. At higher O$_2$ concentration levels (8000 ppm), N$_2$O selectivity became larger than N$_2$ selectivity.

Fig. 2 shows the effect of reaction temperature (120–400 °C) on NO–NH$_3$–O$_2$ reaction on reduced 1%Gd–2%Pd/TiO$_2$. The inlet concentrations of NO, NH$_3$, and O$_2$ are 1800, 1800, and 4000 ppm, respectively. The NH$_3$ conversion increased from 19 to near 100% between 125 and 200 °C. Also, NO conversion reached a maximum value at 200 °C. The O$_2$ conversion remained very low below 5% up to 200 °C; however, it started increasing above 200 °C. The increase in NH$_3$ conversion is partly due to ammonia oxidation reaction above 200 °C.

When the extent of direct ammonia oxidation was examined using 1600 ppm NH$_3$ and 2000 ppm O$_2$, we obtained near complete conversion of ammonia even at temperatures as low as 200 °C. The product
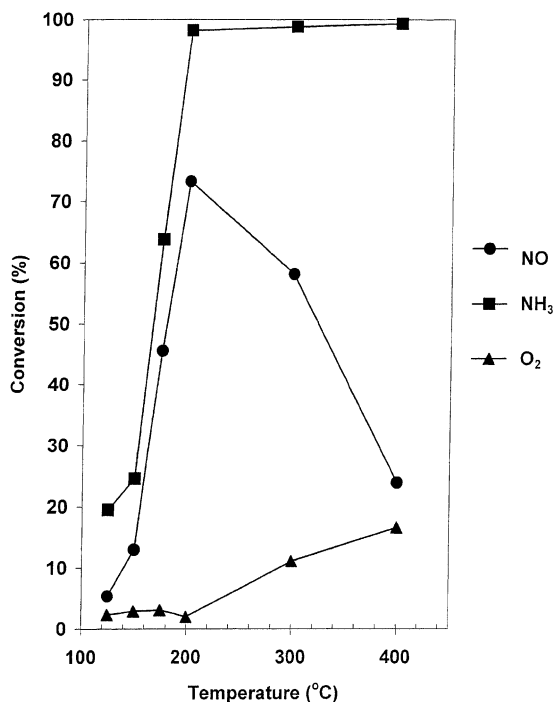
Fig. 2. Effect of temperature on $NO–NH_3–O_2$ reaction on reduced $1\%Gd–2\%Pd/TiO_2$ (NO, NH_3, and O_2: 1800, 1800, and 4000 ppm, respectively).

Table 2
$NO–NH_3$ reaction over reduced and oxidized $Gd–Pd/TiO_2$ at 200 and 250 °C[a]

	NH_3 (200 °C)	NO (200 °C)	NH_3 (250 °C)	NO (250 °C)
Reduced (%)	98	74	97	70
Oxidized (%)	12	8	13	9

[a] NO: 1800 ppm, NH_3: 1800 ppm, 4900 ppm on $Gd–Pd/TiO_2$.

distribution showed an increase in NO formation with increasing temperature, where at 400 °C, the NO yield was around 13%. The only other N-containing product besides NO was N_2O. This result shows that the sharp decline observed in the NO conversion with increasing temperature was not only due to the fact that higher temperatures favor direct NH_3 oxidation over NO reduction, but also due to formation of NO from direct conversion of NH_3 to NO.

In another set of experiments, reduced and oxidized catalysts were compared in NO reduction reaction with NH_3 in the presence of O_2 at 200 and 250 °C. The NO and NH_3 concentrations were 1800 ppm each and the O_2 concentration was 4900 ppm (Table 2). Over the oxidized catalyst, both NO and NH_3 conversion

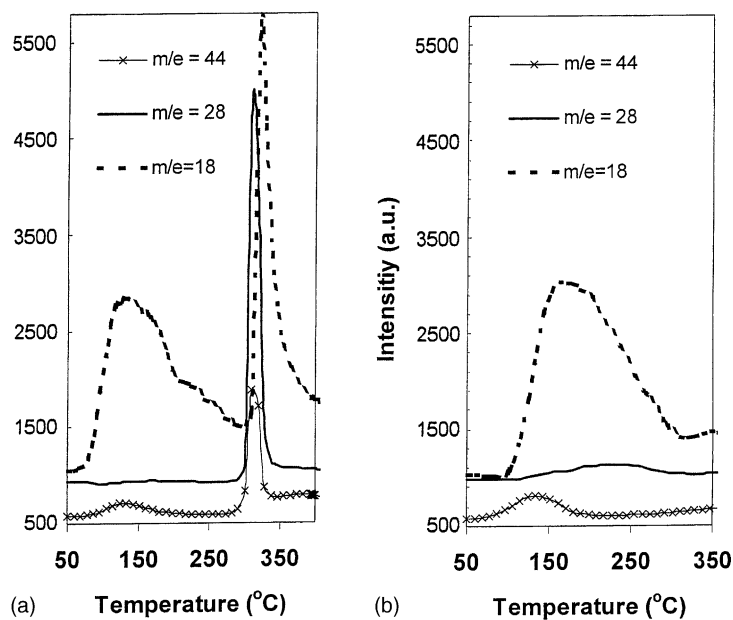

Fig. 3. N_2O-, N_2-, and H_2O-TPD profiles after NH_3 was adsorbed at room temperature on: (a) oxidized $1\%Gd–2\%Pd/TiO_2$ and (b) reduced $1\%Gd–2\%Pd/TiO_2$.

levels were much lower than those obtained over the reduced catalysts. These results suggest that reduced Pd sites are needed for NO–NH$_3$ reaction to proceed over the Gd–Pd/TiO$_2$ catalysts. One possible explanation for the low activity over the oxidized catalyst may be related to NH$_3$ activation, which, analogous to CH$_4$ activation, could require reduced Pd sites. Another explanation may be related to the formation of Pd–NO species, which have been suggested to be the primary species that react with the NH$_x$ species. Our previous studies with in situ DRIFTS have shown Pd–NO species to form primarily over the reduced sites of Pd.

3.2. NH$_3$-TPD

NH$_3$-TPD experiment was performed on oxidized and reduced 1%Gd–2%Pd/TiO$_2$ catalysts. Fig. 3a shows the N$_2$O and N$_2$ desorption profiles ($m/e = 44$ and 28, respectively) following NH$_3$ adsorption on the oxidized sample. The catalyst was calcined in situ in 10% O$_2$ in He for 30 min at 500 °C and cooled to room temperature for NH$_3$ adsorption for 1 h. Then, the catalyst was flushed in He for 1 h before heating at a rate of 10 °C/min.

Over the oxidized catalyst (Fig. 3a), there was a large N$_2$ desorption peak at around 320 °C indicating a strong interaction of NH$_3$ with the catalyst surface. The N$_2$O desorption peaks were observed at 133 and 320 °C. The latter peak coincided with the N$_2$ desorption peak. There were a broad low-temperature water desorption feature (between 60 and 250 °C) and a much sharper high temperature peak (325 °C). The latter feature coincided with desorption of N$_2$ peak, indicating that the formation of nitrogen was coupled with the reduction of the surface by NH$_3$. Over CuO–TiO$_2$-based catalysts, the catalytic oxidation of ammonia to N$_2$ by oxygen has been proposed to occur through formation of hydrazine (N$_2$H$_4$) after molecularly adsorbed NH$_3$ is activated through hydrogen abstraction [3]. However, Burch and co-workers [26] recently showed that bidentate nitrate species, with IR bands at 1546/1280 cm^{-1}, could be an intermediate for N$_2$ formation during temperature-programmed oxidation of NH$_3$. They also studied N$_2$H$_4$ as a probe molecule using DRIFTS and found that neither the thermal stability nor the IR bands correspond to the studied reaction [26].

In our previous XPS studies over oxidized Gd–Pd/TiO$_2$, XPS Pd 3d spectrum showed that nearly all Pd was in +2 oxidation state after the catalyst was treated with O$_2$ at 500 °C [25]. It is possible that NH$_3$ is adsorbed on the oxide surface and oxidized by the surface oxygen, leaving the surface with oxygen vacancies. Additional evidence, which supports involvement of surface oxygen, is the desorption feature of water whose temperature maximum coincided with that of N$_2$ desorption. Although, our previous studies [27] have shown that oxygen in the TiO$_2$ lattice/surface becomes more accessible when a precious metal is supported on the TiO$_2$ surface, we believe reduction of PdO to Pd takes place at significantly lower temperatures than TiO$_2$ reduction, therefore the water formation around 300 °C is the result of the PdO conversion to Pd.

Desorption profiles from NH$_3$-TPD on the reduced Gd–Pd catalyst are presented in Fig. 3b. The catalyst was calcined in situ in 10% O$_2$ in He for 30 min at 500 °C followed by in situ reduction in 33% H$_2$ in He for 30 min at 200 °C before NH$_3$ adsorption at room temperature. After our standard reduction step, majority of PdO is converted to Pd in zero oxidation state as previously shown through XPS data [23]. Therefore, we expected desorption of N$_2$ and N$_2$O to be much smaller compared to the oxidized sample since both reactions involved use of oxygen from the catalyst lattice. As expected, the N$_2$ and N$_2$O features observed on the oxidized sample at 320 °C were not present on the reduced sample. However, the same low-temperature feature was observed on the reduced sample. The broad water desorption feature is likely to be due to water left on the surface from the reduction step.

Fig. 4 shows desorption profiles of NH$_3$ ($m/e = 15$) on both reduced and oxidized samples. Since the parental ion for ammonia of 17 is also a fragment of water ion, we cannot distinguish desorption features of ammonia and water by using $m/e = 17$. Therefore, we used $m/e = 15$ which does not overlap with any other ions. We can see that NH$_3$ adsorbs both reversibly and irreversibly on both samples. The main difference between the two profiles was that the high temperature feature (320 °C) was observed on the reduced sample, but it was absent on the oxidized sample. The temperature at which N$_2$ peak was observed on the oxidized sample matched exactly with the sharp
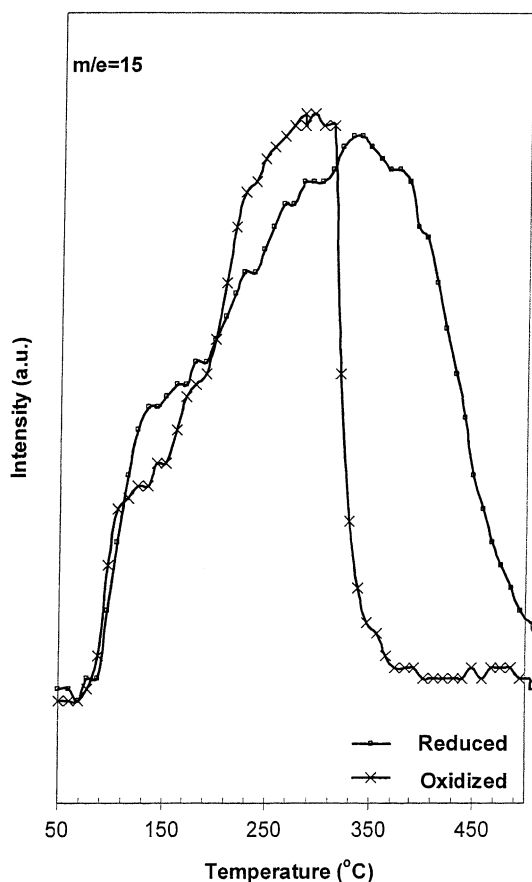
Fig. 4. NH₃-TPD profiles after NH₃ adsorption at room temperature on reduced and oxidized 1%Gd–2%Pd/TiO₂.

drop in the NH₃ feature on the same sample. On the reduced sample, the NH₃ adsorption was mostly reversible, with ammonia desorbing without being transformed to other compounds.

3.3. NH₃ adsorption with DRIFTS

Surface species formed as a result of NH₃ adsorption were examined using DRIFTS. Background spectra were taken at each temperature level that sample spectra were taken after pre-treatment in either H₂/He or O₂/He mixtures. Adsorption of ammonia (3000 ppm in He) was carried out at room temperature for 30 min followed by He flushing. Fig. 5 shows spectra taken over the reduced Gd–Pd/TiO₂ catalyst under NH₃ flow and during the subsequent TPD in He

flow. We observed two strong IR characteristic bands for NH₃ adsorption on Lewis acid sites at 1587 and a doublet at 1176 and 1220 cm⁻¹ (Fig. 5a) These bands correspond to $\delta_{as}(NH_3)$ and $\delta_{sy}(NH_3)$ vibrations of coordinatively adsorbed ammonia, respectively [9,28]. The latter band is located on β Lewis acid sites which are five-coordinated Ti^{4+} sites [28]. The feature at 1220 cm⁻¹ signaled the splitting of the symmetric deformation mode and is reported to be most sensitive to the acidic strength of the surface sites [9]. The strong presence of this band on the reduced Gd–Pd/TiO₂ catalyst, therefore, indicated that NH₃ was strongly adsorbed on the surface. There was a weak signal for NH₃ adsorption on Brönsted acid sites that were indicated by the band at 1421 cm⁻¹. This band represents asymmetric deformation of ammonium ion (NH_4^+) [3,7,28]. It is known that pure anatase does not possess Brönsted acidity; however, the presence of impurities such as silica or sulfates, could enhance Brönsted acidity [7]. The features observed at 3390, 3340, 3250, and 3140 cm⁻¹ (Fig. 5b) characterize the N–H stretching region that are caused by the splitting of the symmetric deformation band [3]. Also, we observed the 3572 cm⁻¹ band which arose due to N–H stretching of NH^+ species [28]. When the surface was heated under He following NH₃ adsorption, the intensity of all features decreased. However, we did not observe any additional features developing which would indicate a transformation of adsorbed ammonia to other surface species. This observation seems to be consistent with our NH₃-TPD experiment on reduced Gd–Pd/TiO₂ where we did not observe any major nitrogen-containing products except for a small N₂O feature at low temperatures.

The same experiment was performed on the oxidized Gd–Pd/TiO₂. The spectra are presented in Fig. 6. In addition to the species observed on the reduced catalyst, we observed a broad peak at 1673 cm⁻¹, which correspond to symmetric deformation of NH_4^+ on Brönsted acid sites. Compared to the reduced sample in Fig. 5a, the intensity of the bands corresponding to NH₃ on Lewis acid sites (1150 and 1592 cm⁻¹) was lower on the oxidized surface. The band (1220 cm⁻¹) signaling the splitting of the symmetric deformation mode was not observed on the oxidized catalyst. This indicated that the adsorption of molecular NH₃ was much weaker on the oxidized Gd–Pd/TiO₂ than it was over the reduced catalyst. Moreover, the
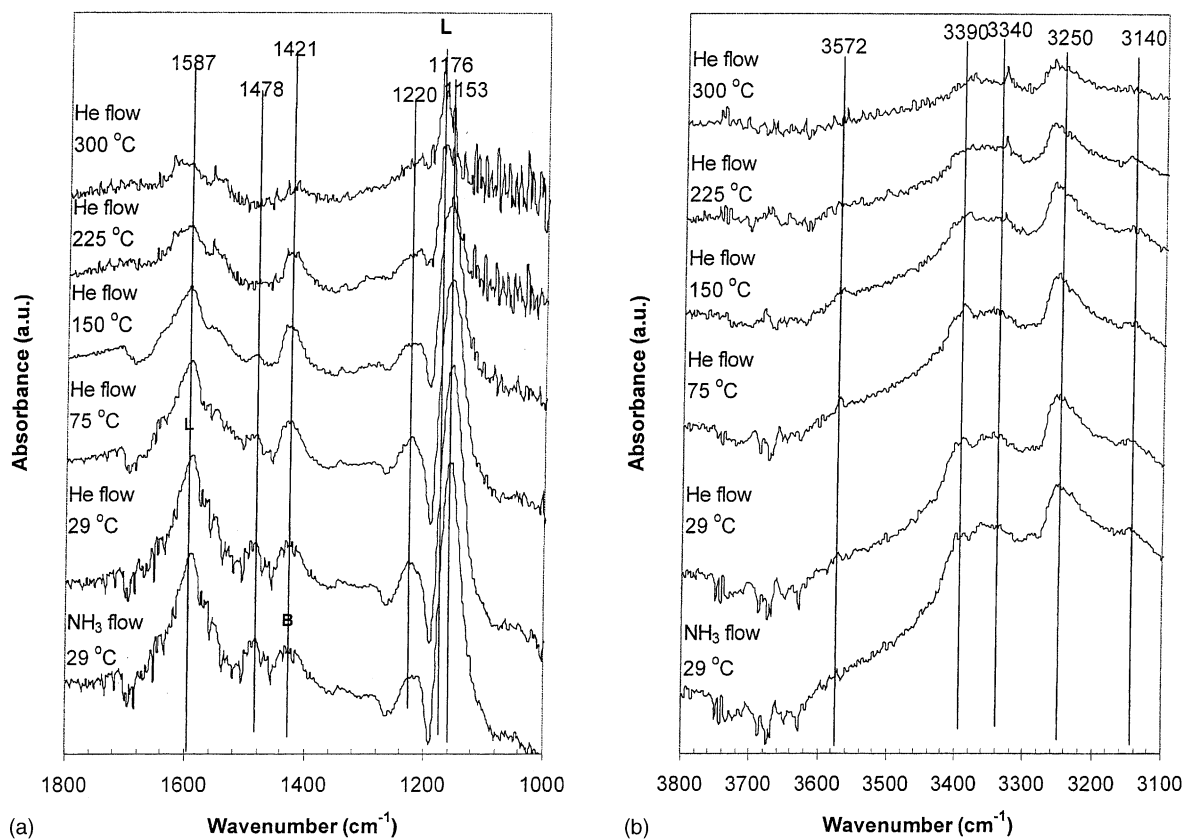
Fig. 5. DRIFT spectra on reduced 1%Gd–2%Pd/TiO$_2$: (a) 1800–1000 cm^{-1} region and (b) 3800–3100 cm^{-1} region.

presence of the bands that characterize Brönsted acid sites (1439 and 1673 cm^{-1}; asymmetric and symmetric deformation modes of NH^{4+}, respectively) seemed to be more pronounced than they were on the reduced sample. In addition, the presence of peaks at 1560 and 1297 cm^{-1} were noticed. The frequencies of these bands seem to correspond to those of monodentate nitrate on titania [29]. The formation of nitrate species indicated that a transformation of adsorbed ammonia took place on the oxide surface. It is plausible that PdO sites could participate in the oxidation of ammonia to nitrate species. When the sample was heated under He, the intensity of all species including the nitrate was reduced, suggesting that they desorb easily with heating. The high-wavenumber regions of the spectra (Fig. 6b) were similar to those observed over the reduced catalysts, except for a decrease in intensity (e.g., 3337 cm^{-1}).

The presence of Gd was found to enhance the catalytic activity for the NO reduction reaction under more oxidizing conditions compared to the Gd-free catalyst [23]. To examine if there are any major differences between the two catalysts or any distinct features that could be attributed to the presence of Gd, the same experiment was performed over the reduced Pd/TiO$_2$ sample. Fig. 7 presents the spectra taken at different temperature levels under He after NH$_3$ adsorption at room temperature. The same species (molecular NH$_3$ and NH$_4^+$) that were found on the reduced Gd–Pd catalyst were also present on the Gd-free sample. One major difference was that the feature at 1220 cm^{-1} (the splitting of NH$_{3sy}$) was significantly weaker on the reduced Pd/TiO$_2$ catalyst compared to that over the reduced Gd–Pd/TiO$_2$ catalyst, suggesting that the NH$_3$ is adsorbed much more strongly on the
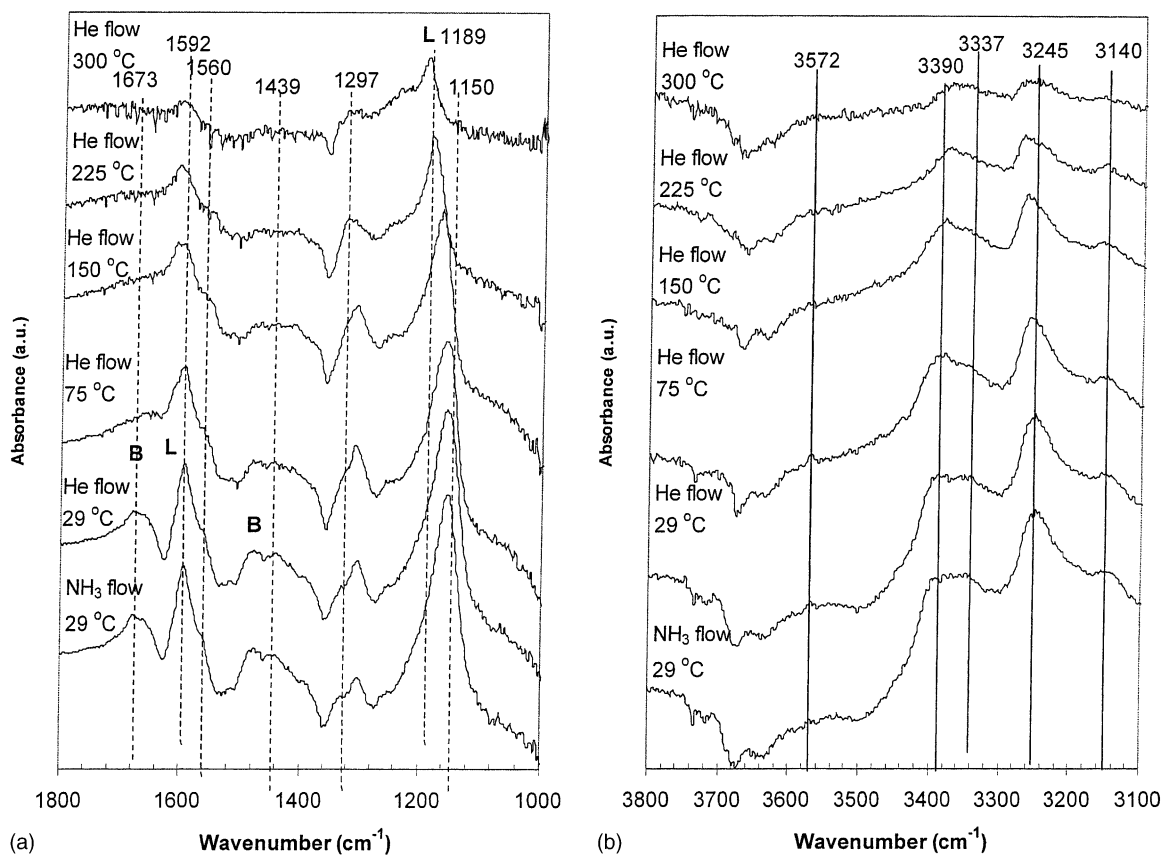
Fig. 6. DRIFT spectra on oxidized 1%Gd–2%Pd/TiO$_2$: (a) 1800–1000 cm^{-1} region and (b) 3800–3100 cm^{-1} region.

Gd-containing catalyst. The surface species and their relative intensities on the reduced Pd/TiO$_2$ catalyst after NH$_3$ adsorption were similar to those on the oxidized Gd–Pd/TiO$_2$. Our earlier studies with in situ DRIFTS under NO–CH$_4$ reaction conditions which have shown that the formation of coordinated NH$_3$ species was more prominent over the Gd–Pd/TiO$_2$ than the Pd/TiO$_2$ catalyst [25] is consistent with the finding that NH$_3$ is more strongly held on the Gd–Pd/TiO$_2$ catalyst. Also, the similarity between DRIFTS spectra of the calcined Gd–Pd catalyst and reduced Pd catalyst following NH$_3$ adsorption could be explained in terms of the electropositivity of the Gd atoms that could be contributing to the electron density of the Pd sites and making them more similar to those found in a partially reduced Gd-free Pd matrix.

3.4. Formation of NH$_x$ species under reaction conditions

The formation of NH$_x$ species on reduced Gd–Pd/TiO$_2$ or Pd/TiO$_2$ catalysts was observed during NO–CH$_4$ reaction at 300 °C. Fig. 8 presents the in situ DRIFT spectra taken over reduced Gd–Pd/TiO$_2$ under flows of NO, NO + CH$_4$, and NO + CH$_4$ + O$_2$, sequentially (NO = 1780 ppm, CH$_4$ = 2.13%, O$_2$ = 2900 ppm) at 300 °C. The catalyst was exposed to the gas mixture for 30 min before each spectrum was taken. Under NO flow, the band at 1793 cm^{-1}, corresponding to NO linearly adsorbed on Pd, was the most prominent feature observed. The weaker bands located around 1535 cm^{-1} represents the formation of nitrate or nitro–nitrito complex [25,29]. Under NO + CH$_4$ flow, where a complete NO conversion
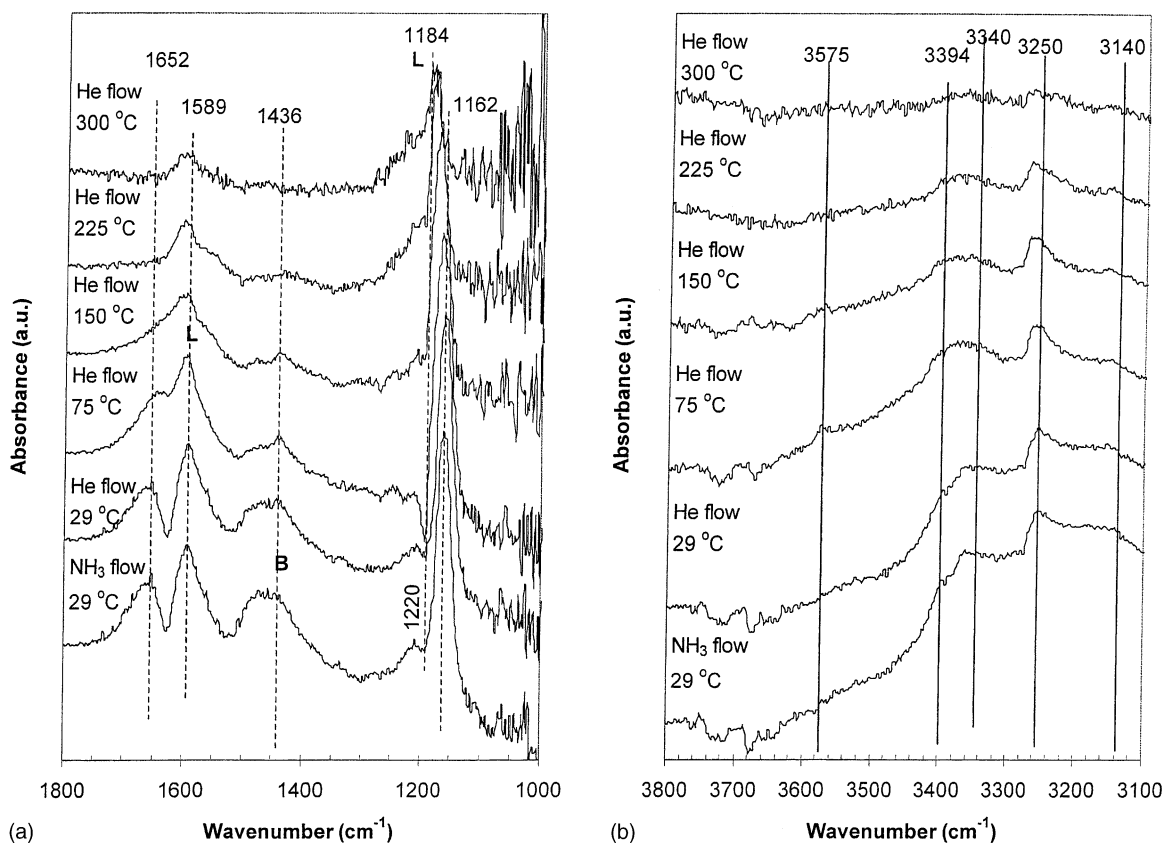
Fig. 7. DRIFT spectra on reduced 2%Pd/TiO$_2$: (a) 1800–1000 cm^{-1} region and (b) 3800–3100 cm^{-1} region.

was achieved, the formation of coordinated ammonia was observed. This species was characterized by the bands at 1186/1220 and 1598 cm^{-1}. In the N–H stretching region, multiplex at 3369 and 3264 cm^{-1} were also observed, indicating the presence of NH$_3$ on Lewis acid sites. Also in the same figure, a complete disappearance of 1793 cm^{-1} band was observed under NO + CH$_4$ flow. When O$_2$ was introduced to NO + CH$_4$ flow, NH$_x$ species seemed to disappear. Concurrently, linear NO species adsorbed on Pd reappeared and the intensity for nitrate species below 1600 cm^{-1} seemed to grow. When CH$_4$ was present in the system, in addition to the characteristics bands for gas-phase methane (1303/3013 cm^{-1}), we also observed bands (2333/2356 cm^{-1}) signaling the formation of CO$_2$.

Fig. 9 shows the spectra taken in a similar experiment where the order in which gases are introduced

to the feed stream was changed from NO $\rightarrow$ CH$_4$ to CH$_4$ $\rightarrow$ NO. It was shown that ammonia was formed and adsorbed on the surface regardless of the order. One difference is that the bands that correspond to NH$_3$ are stronger when the catalyst is exposed to CH$_4$ before NO. This is in agreement with our earlier assertion that NH$_3$ formation requires the initial hydrogen abstraction from CH$_4$, which takes place on Pd^0 sites. Exposing the catalyst to NO flow first may have reduced the number of Pd^0 sites through the partial oxidation of the surface with the O atoms from NO decomposition.

The state of Pd on which linear NO was adsorbed has been discussed in the previous paper [25]. We are of the opinion that linear NO under the reaction conditions could be adsorbed on both metallic (Pd^0) and partially oxidized (Pd$^+$) sites. It was demonstrated that the vibration frequency of Pd–NO may vary in the
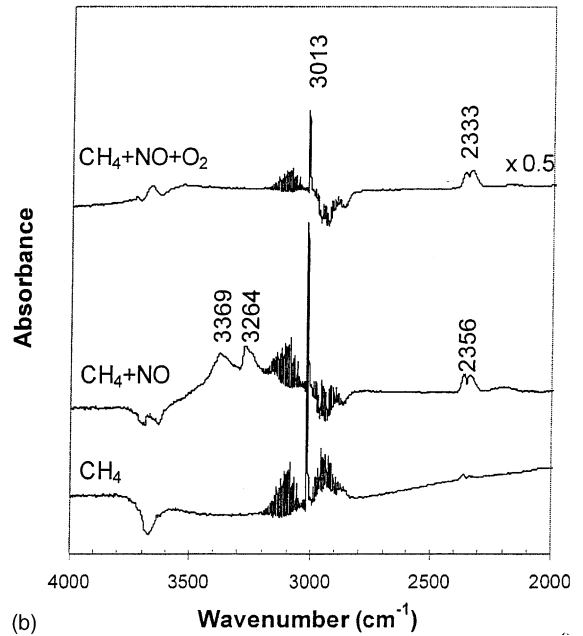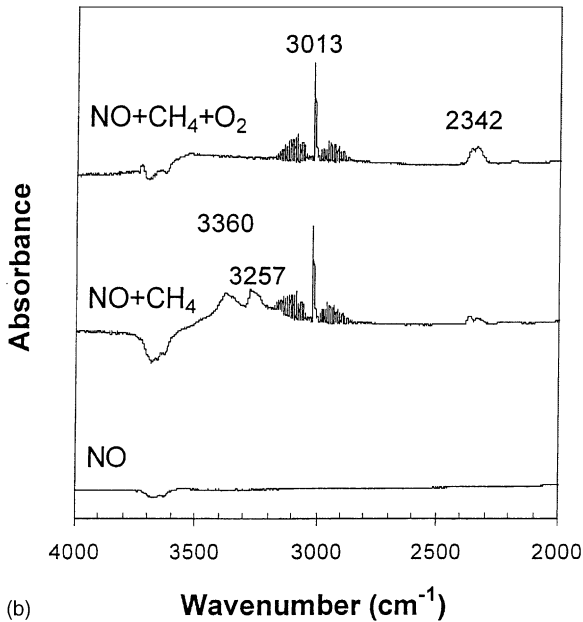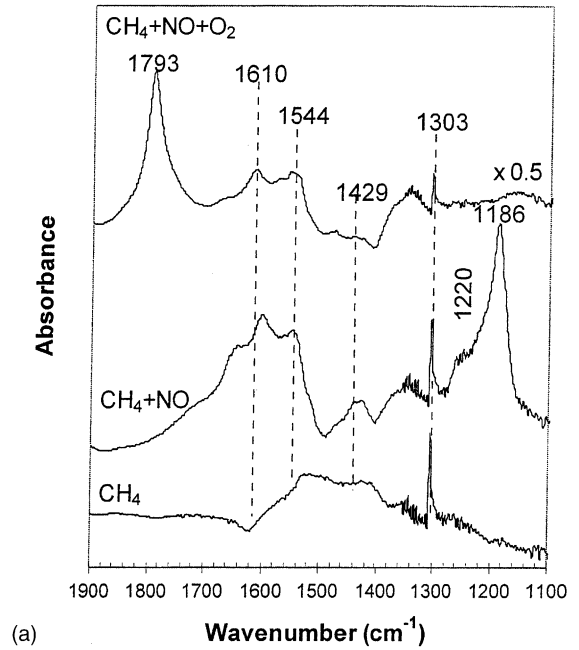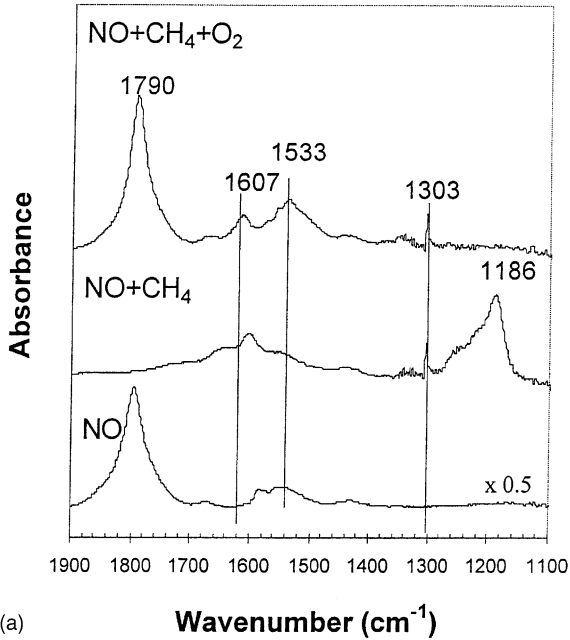
Fig. 8. DRIFT spectra taken over reduced Gd–Pd/TiO$_2$ with sequential addition of the reactants, NO $\rightarrow$ NO + CH$_4$ $\rightarrow$ NO+CH$_4$+O$_2$ (NO = 1780 ppm, CH$_4$ = 2.13%, O$_2$ = 2900 ppm, 300 °C): (a) 1900–1100 cm^{-1} region and (b) 4000–2000 cm^{-1} region.

Fig. 9. DRIFT spectra taken over reduced Gd–Pd/TiO$_2$ with sequential addition of the reactants, CH$_4$ $\rightarrow$ CH$_4$ + NO $\rightarrow$ NO+CH$_4$+O$_2$ (NO = 1780 ppm, CH$_4$ = 2.13%, O$_2$ = 2900 ppm, 300 °C): (a) 1900–1100 cm^{-1} region and (b) 4000–2000 cm^{-1} region.

range from 1750 to 1793 cm^{-1} depending on the surface oxygen concentration. Since oxygen is more electronegative than Pd, the presence of surface oxygen reduces the electron density at Pd atoms. Consequently, fewer electrons are available for backbonding to the antibonding orbital of NO which, in turn, weakens the bond strength between Pd and N-atom of NO [30,31]. Similar results and conclusions have been obtained by Almusaiteer and Chuang [32] when they studied the NO + CO reaction on Pd/Al$_2$O$_3$ using in situ FTIR.

4. Conclusions

Our previous studies [24,25] on sol–gel-prepared Pd catalysts for reduction of NO with CH$_4$ suggested that one of the key surface species for the NO–CH$_4$–O$_2$ reaction involved NH$_x$ species in which case, NO reduction could proceed via in situ SCR-NH$_3$ mechanism. In this study, the use of NH$_3$ as the reducing agent for NO reduction on the Gd–Pd/TiO$_2$ catalyst was investigated under steady-state conditions. It was found that NH$_3$ was effective in reduction of NO over the reduced catalyst. This result was consistent with our earlier suggestion that NH$_x$ species formed through the interaction of methane and the adsorbed NO species on the surface could act as a reducing agent for Pd–NO species. In the presence of O$_2$, however, NH$_3$ oxidation, which has a higher activation energy, becomes more dominant at higher temperatures compared to NO reduction and the observed NO conversion decreases. Our NH$_3$-TPD experiments indicated that the reversible NH$_3$ adsorption capacity was higher on the reduced catalyst compared to the oxidized catalyst. Also, there was a strong evidence provided by DRIFTS that adsorbed NH$_3$ is transformed into monodentate nitrate species on the oxidized catalyst. The literature points to the possibility that the key reaction intermediate for NH$_3$ oxidation to N$_2$ is nitrate species [26].

The better catalytic performance of reduced catalyst could be partially attributed to the fact that coordinatively adsorbed ammonia on Lewis acid sites is more strongly held over the reduced surface than over the oxidized surface. The formation of this species under NO + CH$_4$ flow was achieved only over the reduced catalyst, suggesting that CH$_4$ activation, which is an essential step for ammonia formation, occurs on metallic Pd sites. In the presence of CH$_4$, NH$_x$ species could be formed through an interaction of CH$_x$ with nitrogen-oxo species such as monodentate nitrate, nitro-species, or linear NO on Pd. We observed that NH$_x$ and linear NO species were never present on the surface concurrently. These results strongly suggest that NO reduction to N$_2$ takes place through reduction of Pd–NO species by NH$_x$ and CH$_x$, both of which may function as a reducing agent.

Acknowledgements

References

[1] H. Bosch, F. Janssen, Catal. Today 2 (1988) 369.
[2] U.S. Ozkan, Y. Cai, M.W. Kumthekar, J. Catal. 149 (1994) 375.
[3] G. Ramis, L. Yi, G. Busca, M. Turco, E. Kotur, R.J. Willey, J. Catal. 157 (1995) 523.
[4] G.L. Bauerle, S.C. Wu, K. Nobe, Ind. Eng. Chem. Prod. Res. Dev. 14 (4) (1975) 268.
[5] F.J.J.G. Janssen, Kema Sci. Tech. Rep. 6 (1) (1988) 1.
[6] M. Inomata, A. Miyamoto, Y. Murakami, J. Catal. 62 (1980) 140.
[7] G. Busca, H. Saussey, O. Saur, J.C. Lavalley, V. Lorenzelli, Appl. Catal. 14 (1985) 245.
[8] U.S. Ozkan, Y. Cai, M.W. Kumthekar, J. Catal. 149 (1994) 390.
[9] G. Ramis, L. Yi, G. Busca, Catal. Today 28 (1996) 373.
[10] R.Q. Long, R.T. Yang, Appl. Catal. B 27 (2000) 878.
[11] L.D. Acqua, I. Nova, L. Lietti, G. Ramis, G. Busca, E. Giamello, Phys. Chem. Chem. Phys. 2 (2000) 4991.
[12] U.S. Ozkan, Y. Cai, M.W. Kumthekar, J. Catal. 142 (1993) 182.
[13] R. Burch, F.J. Urbano, P.K. Loader, Appl. Catal. A 123 (1995) 173.
[14] Y. Li, J.N. Armor, Appl. Catal. B 3 (1994) 275.
[15] Y. Nishizaka, M. Misono, Chem. Lett. 1295 (1993).
[16] E. Kikuchi, M. Ogura, I. Terasaki, Y. Goto, J. Catal. 161 (1996) 465.
[17] L.J. Lobree, A.W. Aylor, J.A. Reimer, A.T. Bell, J. Catal. 169 (1997) 188.
[18] D.B. Lukyanov, E.A. Lambardo, G.A. Sill, J.L. d'Itri, W.K. Hall, J. Catal. 163 (1996) 447.
[19] T. Sun, M.D. Fokema, J.Y. Ying, Catal. Today 33 (1997) 251.
[20] E.A. Lambardo, G.A. Sill, J.L. D'itri, W.K. Hall, J. Catal. 173 (1998) 440.

[21] M.W. Kumthekar, U.S. Ozkan, J. Catal. 171 (1997) 54.
[22] U.S. Ozkan, M.W. Kumthekar, G. Karakas, J. Catal. 171 (1997) 67.
[23] J. Mitome, E. Aceves, U.S. Ozkan, Catal. Today 53 (1999) 597.
[24] G. Karakas, J. Mitome-Watson, U.S. Ozkan, Catal. Commun. 3 (2002) 199.
[25] J.M. Watson, U.S. Ozkan, J. Catal., in press.
[26] M. Amblard, R. Burch, B.W.L. Southward, Catal. Today 59 (2000) 365.
[27] U.S. Ozkan, M.W. Kumthekar, G. Karakas, Catal. Today 40 (1998) 3.
[28] M. Kantcheva, V. Bushev, D. Klissurski, J. Catal. 145 (1994) 96.
[29] K. Hadjiivanov, V. Bushev, M. Kantcheva, D. Klissurski, Langmuir 10 (1994) 464.
[30] C.M. Grill, R.D. Gonzalez, J. Phys. Chem. 84 (1980) 878.
[31] S. Moriki, Y. Inoue, E. Miyazaki, I. Yasumori, J. Chem. Soc. Faraday Trans. 78 (1982) 171.
[32] K. Almusaiteer, S.S.C. Chuang, J. Catal. 184 (1999) 189.